

# Artificial Neural Networks and Multiple Linear Regression in Pavement Deterioration Forecasting

Krishna Singh Basnet<sup>1</sup>, Jagat Kumar Shrestha<sup>2</sup>, Rabindranath Shrestha<sup>3</sup>

<sup>1</sup>Institute of Engineering, Tribhuvan University, [krishnasinghasnet@gmail.com](mailto:krishnasinghasnet@gmail.com)

<sup>2</sup>Institute of Engineering, Tribhuvan University, [jagatshrestha@ioe.edu.np](mailto:jagatshrestha@ioe.edu.np)

<sup>3</sup>Institute of Engineering, Tribhuvan University, [rabindra@ioe.edu.np](mailto:rabindra@ioe.edu.np)

---

## Abstract

Assessing pavement conditions in Nepal is costly and time-consuming, with rising traffic and aging infrastructure making maintenance increasingly challenging. This study developed and compared pavement deterioration models to predict the Surface Distress Index (SDI) without manual assessment, using historical road data. SDI was modeled as a function of five key factors: International Roughness Index (IRI), pavement age, total annual rainfall, annual temperature range, and commercial vehicle traffic. Data were collected from relevant government sources, covering 157 road sections with a combined length of 15,783 km, for the period from 2012 to 2022. Multiple Linear Regression (MLR) and Artificial Neural Network (ANN) models were developed for SDI prediction. MLR analysis, conducted in Microsoft Excel, assessed statistical significance through ANOVA,  $R^2$  values, and regression coefficients. In contrast, ANN modeling utilized a Multi-Layer Perceptron (MLP) architecture implemented in TensorFlow and Keras. The ANN model was optimized through iterative experimentation with varied architectures, employing ReLU activation and the Adam optimizer for adaptive learning. The study evaluated a range of architectures, beginning with simple single-layer networks and extending to Deep Neural Networks (DNNs) with up to four hidden layers. Results showed that, during model development, MLR achieved an  $R^2$  of 0.735, whereas the ANN model, with a 5-232-1 structure and 104 epochs, outperformed MLR with an  $R^2$  of 0.809. Validation of both models indicated strong alignment between observed and predicted values, with ANN demonstrating superior predictive accuracy ( $R^2 = 0.816$ ) compared to MLR ( $R^2 = 0.74$ ). The error histogram further confirmed ANN's better performance, which confirms its improved reliability. The study highlights the effectiveness of both models while emphasizing ANN's advantage in capturing complex nonlinear relationships. These findings suggest that integrating ANN into Nepal's pavement management framework can enhance predictive accuracy, reduce assessment costs, and support more efficient maintenance planning.

*Keywords: Pavement, Surface Distress Index, International Roughness Index, Multiple Linear Regression, Artificial Neural Network*

---

## 1. Introduction

Efficient pavement management is essential for sustaining transport networks that promote economic and social development. Pavement Management Systems (PMS) offer a structured approach to plan maintenance, repair, and rehabilitation (M&R), optimizing limited resources and enhancing safety (Abaza et al., 2004; Ferreira et al., 1999; Kulkarni & Miller, 2003; Mathavan et al., 2015; Zakeri et al., 2017). A well-implemented PMS maintains serviceability, structural integrity, and cost-effectiveness while minimizing environmental and social impacts (Fwa et al., 2000). Core PMS components include a road database, condition assessment, cost and performance models, and a Maintenance Optimization System (MOS). The MOS guides M&R strategies using prioritization (Kulkarni et al., 2004; Wong et al., 2003) or optimization models (Abaza, 2006; Durango-Cohen & Tadepalli, 2006; Meneses et al., 2013; Picado-Santos et al., 2004). Understanding pavement deterioration enables better timing of interventions, reducing costs and preserving condition. Performance prediction models are key to determining optimal intervention times (Kerali et al., 2000).

In Nepal, the Department of Roads (DoR) is responsible for the management of 11,179 km of National Highways (NH) (DoR, 2022). The Nepalese government allocates an approximate budget of NRs 7 billion for maintenance. The DoR uses the Annual Road Maintenance Plan (ARMP) as a part of its PMS (DoR, 2007). The DoR collects IRI, SDI, and traffic data to develop the integrated ARMP using a 1995 empirical method

Corresponding Author's Email Address [Krishnasinghasnet@gmail.com](mailto:Krishnasinghasnet@gmail.com)

(Department of Roads & Maintenance Branch, 2005). Presently, IRI is measured on-site, while SDI requires time-consuming videography analysis, leading to higher costs. In 2022, 73% of NHs were in fair to good condition (SDI: 0-3) (Highway Management Information System-Information & Communication Technology (HMIS-ICT) Unit, 2022), but aging infrastructure and rising traffic make it challenging to maintain over 95% of the network in good condition. To address these challenges, a pavement deterioration model is required to simplify data collection, optimize budget allocation, and enhance long-term maintenance planning. Nepal's PMS lacks a performance prediction model, relying instead on annual IRI and SDI assessments, which are labor-intensive, costly, and time-consuming. This reactive approach delays maintenance decisions and reduces efficiency. Manual prioritization, combined with a limited annual maintenance budget of NRs 7 billion, further constrains effective planning. Research on pavement deterioration in Nepal is scarce and often omits key variables. A study in 2021 analyzed relationships between IRI, Pavement Condition Index (PCI), and SDI using regression, but their study had a small sample size and excluded critical factors such as pavement age, traffic, and environmental conditions (S. Shrestha & Khadka, 2021). Sigdel & Pradhananga (2021) developed an IRI model using data from 1,745 road sections, incorporating variables like rainfall and commercial vehicles. However, traffic data were sourced from only 160 stations, raising concerns about accuracy and representativeness. Pavement age, a crucial factor, was also omitted. Although Sigdel et al. (2024) later applied an ANN model, issues with traffic data and age remained unresolved. Similarly, Shakya et al. (2023) used a Markov hazard model but excluded factors such as axle loads, traffic, and climate variables.

This study developed pavement deterioration models to forecast SDI without manual assessment, using a road condition dataset from 2012 to 2022, which uses readily available data to estimate pavement lifespan, support life-cycle cost analysis, and enhance performance prediction. The study employs both MLR and ANN to build the model and compares their effectiveness in predicting SDI.

## 2. Literature Review

Performance prediction models/Deterioration models are used to forecast the future condition, functionality, or service level of an asset. Prediction models are classified into three sub-categories: deterministic, probabilistic, and machine learning. Deterministic models use fixed mathematical equations to predict outcomes, while probabilistic models rely on probability distributions to estimate the likelihood or range of possible future conditions (Anyala et al., 2014; Sanabria et al., 2017; Wang et al., 2017). The empirical method is one of the deterministic models that apply statistical analysis to key deterioration factors like pavement age and traffic load, often using linear or nonlinear regression techniques (Anyala et al., 2014). Univariable regression analyses a single factor, whereas multivariable regression considers multiple variables. Given the complexity of asset deterioration, univariable models often lack accuracy compared to multivariable approaches. The regression modelling process starts with data collection and quality checks, followed by diagnostics to explore variable relationships and interactions. If issues are found, remedial measures like data transformation are applied. Relevant explanatory variables are selected, and interaction or non-linear effects are further analysed. Residuals and diagnostics help assess model fit, with additional corrections if needed. A tentative model is then chosen and validated. If it meets assumptions and performs well, it becomes the final regression model. This iterative process ensures accuracy and reliability (Neter et al., 1996). Regression models are flexible and easy to use, allowing for various functional forms to analyze data. Their performance is typically evaluated using statistical metrics that measure fit quality. While the coefficient of determination ( $R^2$ ) is commonly used, some researchers advocate for error-based metrics, such as percentage errors, to better assess model accuracy (Arhin & Noel, 2014; Ashrafi et al., 2020; Gong et al., 2019).

ANNs are one of the machine learning models, which are AI-based computational models capable of solving complex, nonlinear engineering problems like pavement condition assessment and prediction (Adeli, 2001). Inspired by the human brain, ANNs process data through interconnected artificial neurons (mathematical analogs of biological neurons) using weighted connections to learn and make decisions (Georgiou et al., 2018; Mosa, 2017). ANNs are increasingly used in pavement performance forecasting, leveraging condition indicators to predict deterioration such as cracking, rutting, or roughness (Bosurgi & Trifirò, 2005; Domitrović et al., 2018). Building an ANN involves defining three core components: (1) the number of layers—a minimum of three: input,

hidden, and output; (2) the number of neurons per layer; and (3) the activation functions and training parameters (Elshamy et al., 2020). Feed-Forward Neural Networks (FFNNs), a common ANN type, operate in one direction without feedback loops. They consist of input, hidden, and output layers, where each neuron computes outputs by applying an activation function to the weighted sum of inputs. FFNNs may be single-layer or multi-layer; the latter includes hidden layers that enable the extraction of complex features (Sazlı, 2006). Fully connected networks link every neuron in one layer to all neurons in the next layer (Haykin, 1998). The Multi-Layer Perceptron Neural Network (MLPNN) is a typical FFNN structure comprising at least one hidden layer. When it includes multiple hidden layers, it is referred to as a Deep Neural Network (DNN). Training adjusts weights via algorithms like gradient descent or Levenberg-Marquardt to minimize prediction error (A. Shrestha & Mahmood, 2019). Rectified Linear Unit (ReLU) is a widely used activation function that mimics the brain's sparse neuron activation—only a small fraction of neurons fire at a time, reducing computational load and overfitting risks. ReLU outputs zero for negative inputs and scales linearly for positives, mirroring biological neuron responses (Glorot et al., 2011; LeCun et al., 2015).

### 3. Methodology

#### 3.1 Variables

The study defined SDI as a function of five independent variables: IRI, pavement age (Age), total annual rainfall (RF), annual temperature range (TD), and Commercial Vehicles per day (CV), with reference to the literature review of several past studies, as shown in the equation 1. The variable Age refers to the number of full years elapsed since the most recent major structural intervention that effectively reset the pavement's deterioration lifecycle. The variable RF represents the cumulative depth of precipitation that occurred during the twelve months preceding the year of prediction. The TD variable denotes the annual temperature range experienced at the road section, calculated as the difference between the average daily maximum and minimum temperatures over a continuous twelve-month period. Lastly, CV indicates the average number of commercial vehicles, specifically trucks (light, heavy, and multi-axle) and buses (large, mini, and micro), passing a road section per day.

$$SDI=f [IRI, Age, RF, TD, CV] \dots\dots\dots (1)$$

#### 3.2 Study Area and Data Collection

This study focused on the national highways of Nepal, which connects major urban centres, trade corridors, and border points. Data were collected from the HMIS of the DoR, the RBN, and the Department of Hydrology and Meteorology (DHM) for the period 2012-2022.

Though SDI/IRI measurements in Nepal began in 1995, a systematic online database was only established in 2012, limiting the study to data from that year onward. Moreover, though there are a greater number of road sections within the SRN, reliable traffic data exist only for 160 sections in the HMIS, as traffic count stations are located on or near these sections (DoR, 2023). Assigning traffic volumes from distant stations could produce misleading estimates because of location variations in access patterns, land use, and traffic composition. Among them, three lacked corresponding roughness data; hence, 157 sections were used for modelling. These sections, averaging 15.7 km in length and totalling 15,783 km (from 2012 to 2022). Therefore, only sections with both direct traffic and surface-condition data were retained to maintain reliability. The road sections and traffic count stations taken for the study are shown in Figure 1. All selected road sections were flexible pavements as listed in the DoR inventory. Although the SRN includes other surface types, sub-type data for flexible pavements have not been consistently recorded since 2012. Therefore, the study treated flexible pavements as a general category representative of Nepal's SRN.

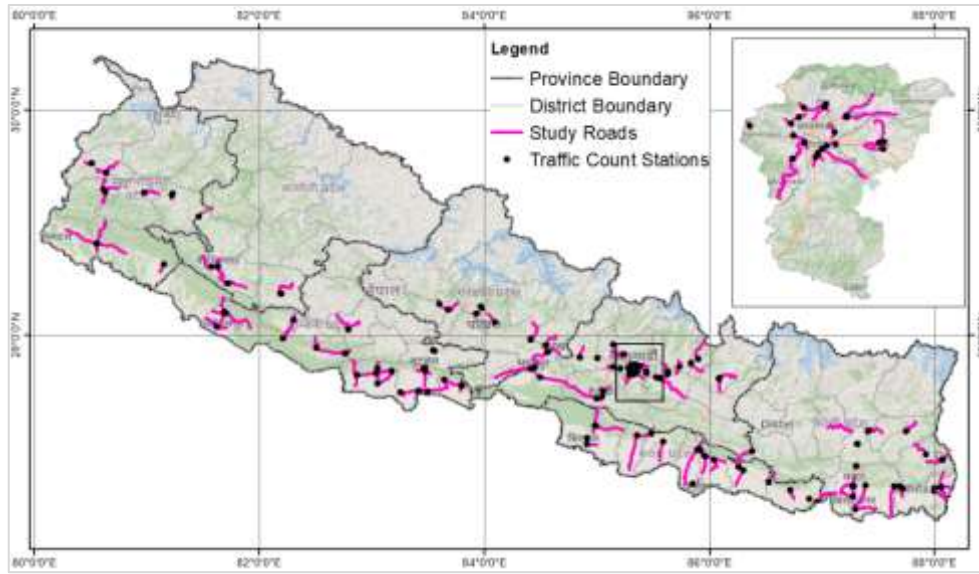


Figure 1 Study Area

Data on SDI, IRI, and traffic were collected from the HMIS (DoR, 2023) as discussed earlier. Climatic variables were obtained from the nearest DHM meteorological stations (Figure 2), which provide the only official long-term climatic records in Nepal. Average annual rainfall and temperature difference were computed for each road section. Despite potential micro-climatic variations, these datasets offer the best available representation of regional climatic influences on pavement deterioration. Due to the unavailability of direct records on pavement age, it was estimated indirectly by identifying abrupt reductions in SDI or IRI values, which typically indicate overlays or major rehabilitation works. These deduced ages were then cross-validated with maintenance and rehabilitation records from the RBN. Pavement age was assigned as zero for years in which major structural improvements were detected.

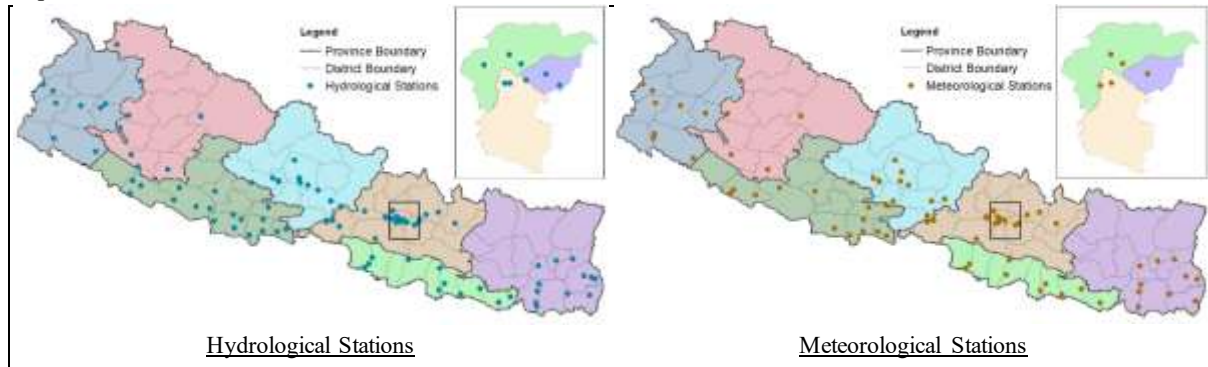


Figure 2 Climate Stations used for the study

### 3.3 Data preprocessing

Before model development, the data were organized and cleaned to remove inconsistencies and outliers. This involved using imputation to fill missing values, allowing incomplete records to be retained, and capping to limit extreme values by replacing them with defined thresholds. These techniques helped maintain the integrity of the dataset. Furthermore, Pearson's correlation coefficients were computed using Microsoft Excel to assess multicollinearity among independent variables.

### 3.4 Multi-linear Regression (MLR)

Multiple linear regression analysis was conducted using Microsoft Excel to establish the relationship between SDI and the specified five independent variables. The dataset was split into two parts: 80% for model development and 20% for validation. The MLR model was built using the development dataset and evaluated on the validation dataset using key performance metrics. The regression aimed to predict the dependent variable (SDI) based on multiple independent variables, using the general model as presented by the equation 2.

$$y = b_0 + b_1x_1 + b_2x_2 + \dots + b_nx_n \dots\dots\dots (2)$$

where,  $y$  is the dependent variable,  $x_1$  to  $x_n$  are predictors, and  $b_0$  to  $b_n$  are regression coefficients. The model's statistical significance and explanatory power were evaluated using ANOVA and the coefficient of determination ( $R^2$ ). ANOVA tested whether the model significantly explained variance in the dependent variable, while  $R^2$  measured the proportion of SDI variance accounted for by the independent variables, indicating goodness-of-fit. Model reliability was verified using the validation dataset, comparing predicted SDI values against observed values to assess predictive performance. Furthermore, k-fold cross-validation was conducted in 5-folds to check the statistical robustness of the model.

### 3.5 Artificial Neural Network (ANN)

In this study, an ANN model was developed using a supervised learning approach to predict the SDI. The full dataset was divided into two subsets: 80% for model development (training and testing) and 20% for validation. Furthermore, k-fold cross-validation in 5-folds was conducted to check the statistical robustness of the model.

The model was developed in Python using TensorFlow, with Keras providing a high-level interface for streamlined construction and training. A MLP was employed to capture complex data relationships through multiple interconnected layers. The model iteratively calculated weight and bias matrices using a feed-forward architecture with backpropagation. During the feed-forward phase, input data passes through hidden layers, where weighted sums are computed and processed via the ReLU activation function,  $f(x)=\max(x,0)$ , introducing non-linearity. The output is compared with actual values to compute error, which is then propagated back to adjust weights. The Adam optimizer was used to adaptively update learning rates, enhancing training efficiency, especially with sparse gradients or noisy data. The iteration process is illustrated in Figure 3.

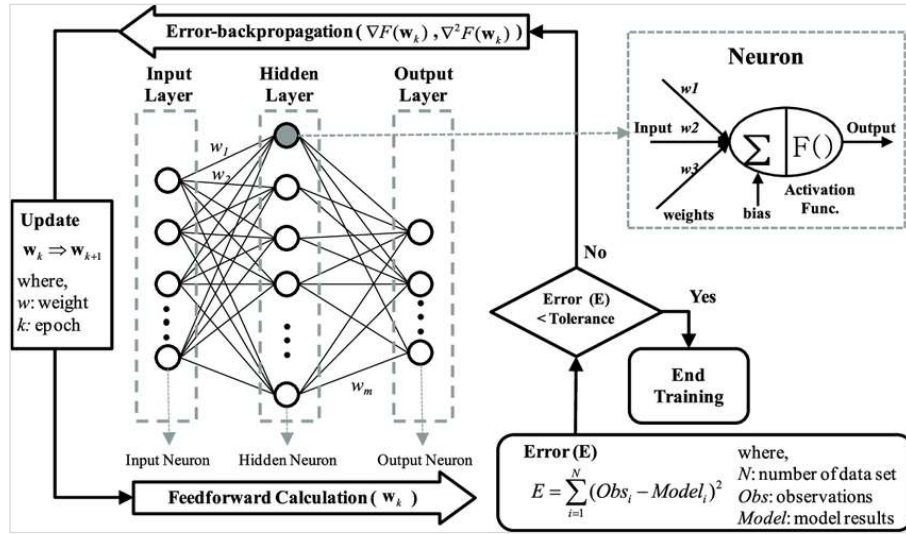


Figure 3 Iteration Process (Kim & Seo, 2015)

The architecture consisted of an input layer with five nodes corresponding to the selected features. Hidden layer configurations were determined through iterative experimentation, testing different combinations of layers and neurons. The optimal architecture was selected based on performance metrics, including  $R^2$  and mean squared error (MSE), with training iterations (epochs) run until the highest  $R^2$  and lowest MSE were achieved. The study explored the performance of ANN with up to two hidden layers and further investigated DNN with up to four hidden layers. The framework for ANN model development is shown in Figure 4.

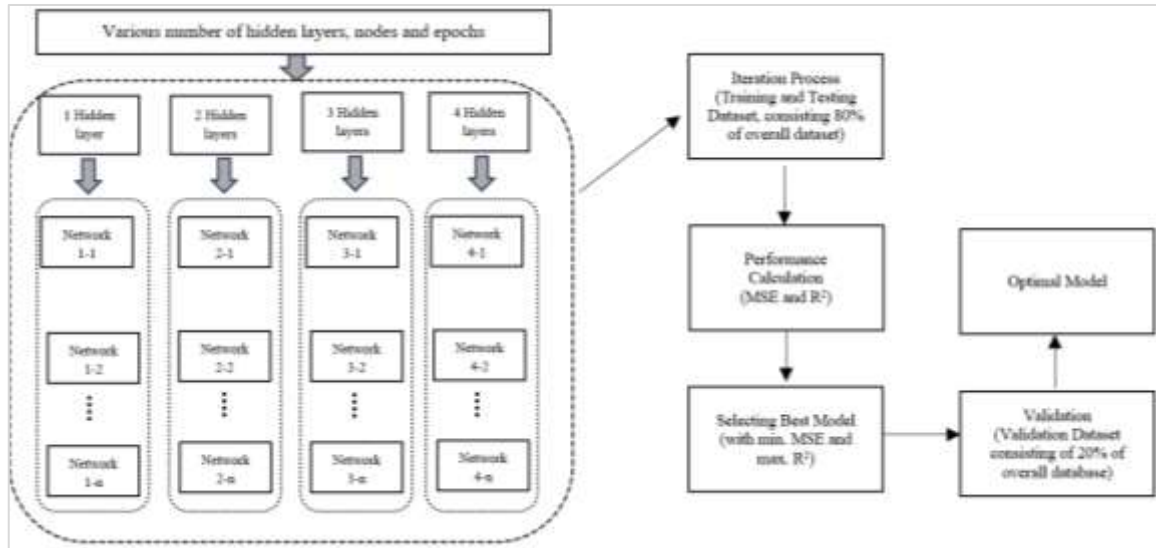


Figure 4 ANN Model Development Framework

Model training involved minimizing the error between predicted and actual SDI values, quantified using the squared error function as presented in the equation 3 while weight updates during backpropagation, following the equation 4.

$$E = \sum_{i=1}^N (\text{Obs}_i - \text{Model}_i)^2 \dots\dots\dots (3)$$

$$W_{\text{new}} = W_{\text{old}} + \alpha * (\text{Obs} - \text{Model}) * x \dots\dots\dots (4)$$

Where, E: Error; Obs: Observed Value; Model: Model Predicted Value;  $\alpha$ : Learning rate; x: Input Value;  $W_{\text{new}}$ : New Weightage;  $W_{\text{old}}$ : Old Weightage.

After training the MLPNN, the model output can be expressed using a specific mathematical formulation. For instance, an MLPNN with a single hidden layer and a single output neuron can be represented as shown in the equation 5 (Yang et al., 2021).

$$\text{Output} = f_0[B_0 + \sum_K W_K f_H(B_{HK} + \sum_i W_i \text{Input}_i)] \dots\dots\dots (5)$$

Where,  $f_0$  and  $f_H$  are activation functions used in the output layer and hidden layer;  $B_0$  and  $B_H$  are biases for the output layer and hidden layer;  $W$  is the weight between the nodes;  $K$  is the number of nodes in the hidden layer; and  $i$  is the number of the input variables.

### 3.6 Sensitivity Analysis

A sensitivity analysis was conducted on the developed prediction models to identify the most and least influential parameters in predicting SDI. The study employed the equation 6 to compute the sensitivity index (Chang & Liao, 2012).

$$S = \left\{ \left( \frac{O_2 - O_1}{I_2 - I_1} \right) * \left( \frac{I_{\text{avg}}}{O_{\text{avg}}} \right) \right\} \dots\dots\dots (6)$$

where, S: Sensitivity Index;  $I_1, I_2$ : Minimum and Maximum Input values respectively;  $O_1, O_2$ : Output values corresponding to  $I_1$  and  $I_2$  respectively;  $I_{\text{avg}}, O_{\text{avg}}$ : Average  $I_1, I_2$  and Average  $O_1, O_2$  respectively.

## 4. Results and Discussion

### 4.1 Multi-Collinearity

Figure 5 illustrates the Pearson correlation heatmap, which revealed coefficients ranging from 0.01 to 0.58, indicating weak to moderate correlations and no significant multicollinearity. Therefore, all five variables were included in the pavement performance prediction model. The correlation between IRI and Age was highest ( $r = 0.58$ ), followed by IRI and Rainfall ( $r = 0.25$ ), both indicating weak relationships.

	IRI	Age	Rainfall	Temp Diff.	CVPD
IRI	1.00	0.58	0.25	0.08	0.22
Age	0.58	1.00	0.23	0.05	0.04
Rainfall	0.25	0.23	1.00	0.01	0.08
Temp Diff.	0.08	0.05	0.01	1.00	0.15
CVPD	0.22	0.04	0.08	0.15	1.00

Figure 5 Pearson Correlation Coefficient Heatmap

## 4.2 MLR

ANOVA test results as presented in Table 1 show an F-statistic of 429.224 with a p-value below 0.05, indicating a statistically significant relationship between SDI and the independent variables. This leads to the rejection of the null hypothesis, confirming the presence of correlations. The degrees of freedom were 5 (regression) and 784 (residual), reflecting five estimated parameters and 784 unexplained data points. The Regression Mean Square (83.5) and Residual Mean Square (0.19) indicate that most variability is explained by the model. Similarly, the Regression Sum of Squares (SSR = 417.6) exceeds the Residual Sum of Squares (SSE = 152.5), suggesting the model captures a substantial portion of the total variance in the dependent variable.

Table 1 ANOVA Results

	Degree of freedom (df)	Sum of Squares (SS)	Mean of Squares (MS)	F Statistics	Significance F (p - value)
Regression	5	417.677	83.535	429.224	1.3153E-221
Residual	784	152.582	0.195		
Total	789	570.259			

Regression statistics, as presented in Table 2, show model quality and accuracy. A Multiple R of 0.856 indicates a strong positive linear relationship between independent and dependent variables. The R-Square value of 0.732 shows that 73.2% of the variation in SDI is explained by the model, while the Adjusted R-Square of 0.731 accounts for the number of predictors. The Standard Error of 0.441 reflects the average deviation of observed values from predicted values, confirming the model's strong fit using the five selected independent variables.

Table 2 Regression Statistics

Regression Statistics	
Multiple R	0.856
R Square	0.732
Adjusted R Square	0.731
Standard Error	0.441
Observations	790

Table 3 presents the coefficients and test statistics from the multiple linear regression analysis. All five predictors: IRI (0.146), Pavement Age (0.167), Rainfall (0.058), Temperature Difference (0.018), and CV (0.052), show positive relationships with SDI. IRI and Age are the most influential, while CV has a moderate impact, likely due to maintenance in high-traffic areas. All predictors are statistically significant ( $p < 0.05$ ), with high t-values and narrow confidence intervals confirming estimate reliability.

Table 3 Test Statistics and Coefficients

	Coefficients	Standard Error	t Stat	P-value	Lower 95%	Upper 95%
Intercept	0.310	0.113	2.749	0.006	0.089	0.531
IRI	0.146	0.009	17.094	0.000	0.129	0.163
Age	0.167	0.007	22.427	0.000	0.152	0.181
RF (in m)	0.058	0.025	2.302	0.022	0.009	0.108
TD (in °C)	0.018	0.082	2.175	0.030	0.017	0.341
CV (in '000 veh)	0.054	0.010	5.197	0.000	0.034	0.074

Based on the outcomes of the multiple linear regression analysis, the model for SDI concerning Nepal's national highway pavements is formulated as the equation 7.

$$\text{SDI} = 0.31 + 0.146 \text{ IRI} + 0.167 \text{ Age} + 0.058 \text{ RF} + 0.018 \text{ TD} + 0.054 \text{ CV} \dots\dots\dots (7)$$

Where, SDI: Surface Distress Index; IRI: International Roughness Index / Performance function (m/Km); Age: Pavement Age in years; RF: Total Rainfall in m; TD: Annual Max and Min Temperature Difference in °C; CV: Number of Commercial Vehicles per Day in thousands (thousand veh.)

For validation, the model was tested on a separate dataset of 189 observations (20% of the total). The  $R^2$  value for validation was 0.7404, slightly higher than the model's training  $R^2$ , indicating that 74.04% of the SDI variance was accurately predicted.

Figure 4.4 shows scatter plots comparing observed and predicted SDI for the model development, validation, and combined datasets. The model performed well in both phases, showing strong correlations and good generalization. The MLR model explains about 73% of the variance in the overall SDI dataset.

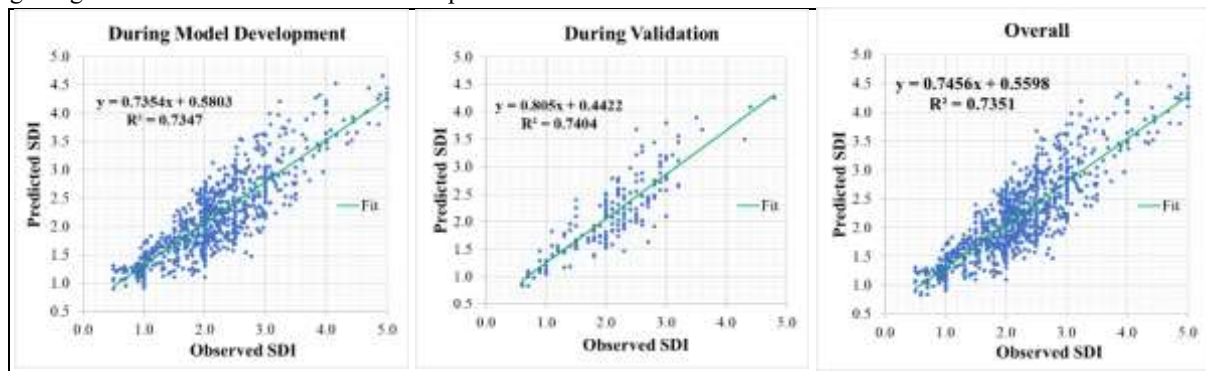


Figure 6 Predicted SDI Vs measured SDI under MLR

The results of the 5-fold cross-validation presented in Table 4 demonstrate the robustness and consistency of the MLR model. The  $R^2$  values range from 0.724 to 0.742, with an average of 0.733, indicating that the model explains approximately 73% of the variation in the SDI. The low variation across folds and the relatively small MSE (0.194) and MAE (0.362) confirm the model's stability.

Table 4 k-fold Cross-validation for MLR

Fold	$R^2$	MSE	MAE
1	0.724	0.202	0.374
2	0.736	0.197	0.36
3	0.729	0.19	0.358
4	0.742	0.186	0.35
5	0.733	0.193	0.365
Mean	0.733	0.194	0.362

#### 4.3 ANN

The study began with a simple ANN architecture using one hidden layer, testing node counts from 32 to 256 and epochs from 32 to 112 (in steps of 8), totalling 319 iterations. This was followed by testing two hidden layers (275 iterations), then three (187 iterations), and finally four (11 iterations), each time recording  $R^2$  and

MSE. As the number of layers and nodes increased, so did the computational demand. Figure 7 summarizes results for one and two hidden layer networks. For one hidden layer, the 5-232-1 architecture achieved the best performance with a minimum MSE of 0.138 and a maximum  $R^2$  of 0.808 at epoch 104. For two hidden layers, the 5-224-32-1 architecture achieved a minimum MSE of 0.139 and  $R^2$  of 0.80 at epoch 72.

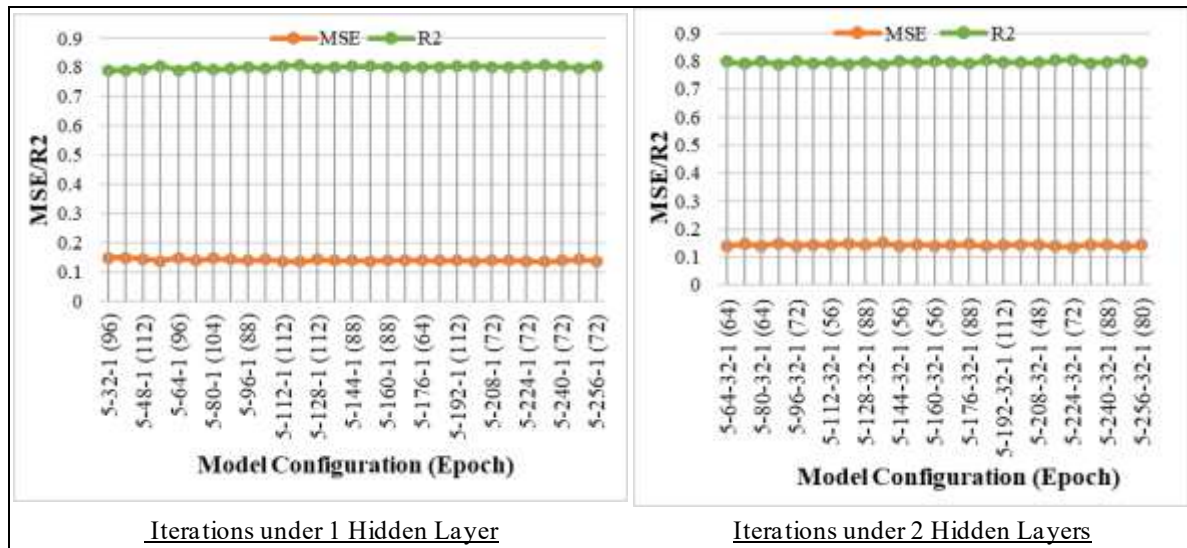


Figure 7 Iterations for Optimum Network Model under ANN

Similarly, Figure 8 illustrates the iterations conducted using a DNN with 3 to 4 hidden layers. For the network with three hidden layers, the architecture 5-208-64-32-1 yielded a minimum MSE of 0.143 and a maximum  $R^2$  of 0.79 at epoch 72. The latter, with the architecture 5-256-128-64-32-1, yielded a minimum MSE of 0.153 and a maximum  $R^2$  of 0.78 at epoch 40.

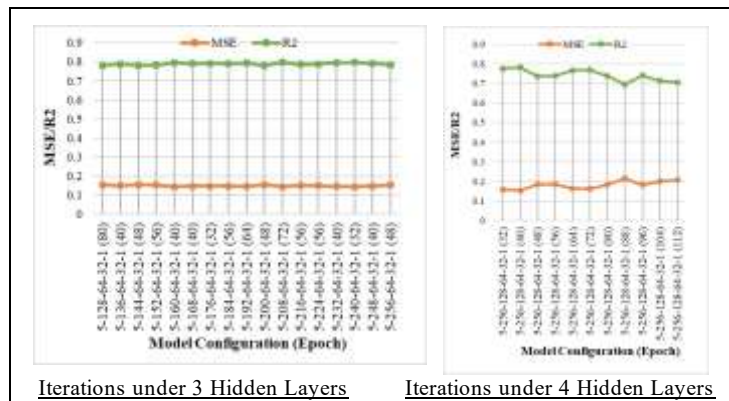


Figure 8 Iterations for Optimum Network Model under DNN

The optimal ANN model was identified as 5-232-1 with 104 epochs, as shown in Figure 9. In the figure, blue dots represent inputs, reddish denotes hidden layers, and green indicates the output. This model demonstrated high computational efficiency, requiring just 2.2 seconds to train on an AMD Ryzen 7 6800H (3.20 GHz) with 16 GB RAM. Given that the dataset spans 10 years and is unlikely to grow significantly, training time remains minimal, making frequent model updates practical.

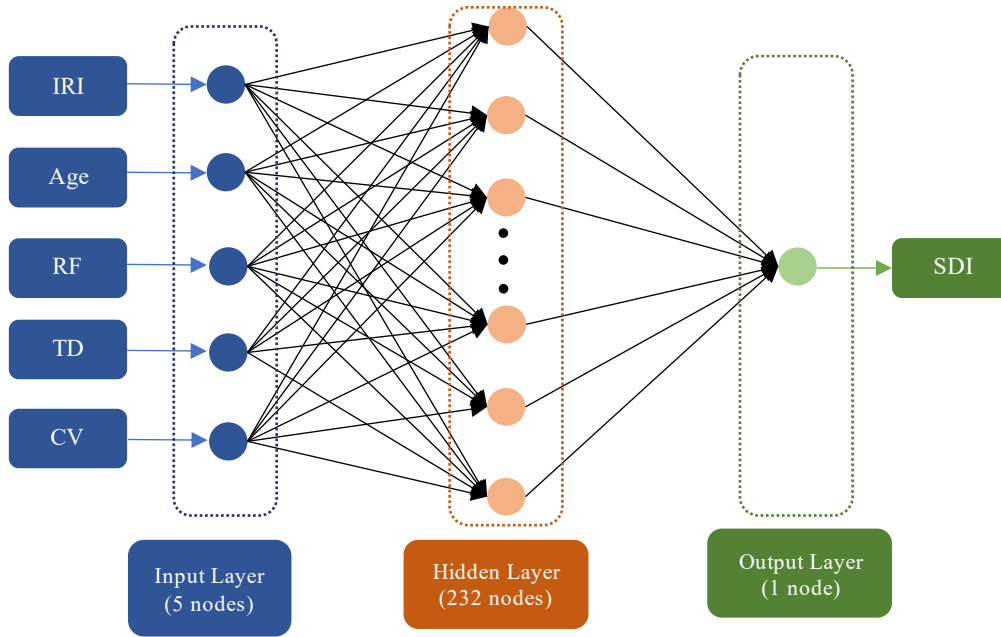


Figure 9 The 5-232-1 NN Model Architecture

The equations for transformations in the hidden layer can be written as the equation 8. The output layer applies a weighted sum of the hidden layer outputs to produce the final output, which can be written as the equation 9. Finally, when combining the transformations in all the layers, the complete equation for the output  $y$  can be written as the equation 10. The model for predicting SDI can be written as the equation 11.

$$h_j = \text{ReLU} \left( \sum_{i=1}^5 W_{1ji} X_i + b_{1j} \right) \dots\dots\dots (8)$$

For  $j = 1, 2, \dots, 232$  nodes in the hidden layer.

$$y = \sum_{j=1}^{232} W_{2j} h_j + b_2 \dots\dots\dots (9)$$

$$y = \sum_{j=1}^{232} W_{2j} \text{ReLU} \left( \sum_{i=1}^5 W_{1ji} X_i + b_{1j} \right) + b_2 \dots\dots\dots (10)$$

$$\text{SDI}_{\text{Predicted}} = W_0 * [W_1 * I + B_1] + B_2 \dots\dots\dots (11)$$

where,  $W_0$  = Output Weight Matrix;  $W_1$  = Input Weight Matrix;  $B_1, B_2$  = Bias Matrix for hidden and Output Layers;  $X_i$  =  $i$ -th input feature (where  $i=1,2,3,4,5$  for IRI, PA, RF, TD, CV respectively);  $W_{1ji}$  = weight from the  $i$ -th input node to the  $j$ -th hidden node;  $b_{1j}$  = bias for the  $j$ -th hidden node;  $h_j$  = output of the  $j$ -th hidden node after applying the ReLU activation function;  $W_{2j}$  = weight from the  $j$ -th hidden node to the output node;  $b_2$  = bias for the output node;  $y$  = predicted SDI

The ANN model was validated using 189 observations (20% of the dataset), achieving an  $R^2$  of 0.816, slightly higher than during training, indicating that 81.6% of the SDI variance was accurately predicted. Figure 10 compares observed and predicted SDI for the training, validation, and overall datasets. The model shows strong correlations and consistent performance across all phases, with minor prediction errors. The ANN model explains about 80% of SDI variability in the overall dataset.

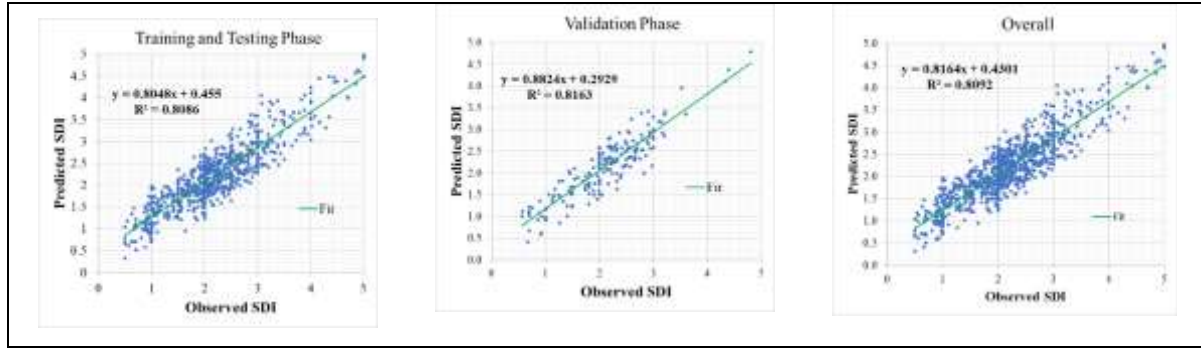


Figure 10 Predicted SDI Vs observed SDI using ANN

The 5-fold cross-validation results in Table 5 confirm the superior performance and reliability of the ANN model. The  $R^2$  values range from 0.799 to 0.817, with an average of 0.809, indicating that the ANN model explains about 81% of the variation in the SDI (a notable improvement over the MLR model). The mean values of MSE (0.134) and MAE (0.292) are consistently lower across all folds, suggesting higher predictive accuracy and better generalization.

Table 5 k-fold Cross-validation for ANN

Fold	$R^2$	MSE	MAE
1	0.799	0.141	0.304
2	0.812	0.134	0.289
3	0.808	0.131	0.295
4	0.817	0.128	0.283
5	0.810	0.136	0.291
<b>Mean</b>	<b>0.809</b>	<b>0.134</b>	<b>0.292</b>

#### 4.4 Comparison

Table 6 and Figure 11 summarize model performance across development, validation, and overall datasets. The MLR model showed decent accuracy with an  $R^2$  of 0.735, MSE of 0.191, and MAE of 0.367 during development. Validation slightly improved with  $R^2$  of 0.740, MSE of 0.141, and MAE of 0.307. In comparison, the ANN model outperformed MLR in all phases. It achieved an  $R^2$  of 0.809, MSE of 0.138, and MAE of 0.301 during development, and improved further in validation ( $R^2 = 0.816$ , MSE = 0.102, MAE = 0.263). ANN showed stronger accuracy and generalization in predicting SDI.

Table 6 Summary of performance evaluation parameters

Model	Eqn. (No.)	Phase/Data Set	No. of Data Set	MSE	MAE	MAPE	MAD	R2	RMSE
MLR	7	Model Development	790	0.191	0.367	19.758	0.192	0.735	0.437
		Validation	189	0.141	0.307	16.573	0.166	0.740	0.375
		Overall	979	0.191	0.367	19.758	0.192	0.735	0.437
ANN	11	Training and Testing (Model Development)	790	0.138	0.301	16.414	0.182	0.809	0.372
		Validation	189	0.102	0.263	15.290	0.150	0.816	0.319
		Overall	979	0.131	0.294	16.197	0.176	0.809	0.363



Figure 11 Comparison of evaluation parameters of developed models

Figure 12 compares error distributions of the developed models, highlighting differences in predictive accuracy. The MLR model shows a wider error spread, indicating higher variance and moderate accuracy. In contrast, the ANN model exhibits a tighter distribution centred around zero, reflecting greater accuracy and consistency.

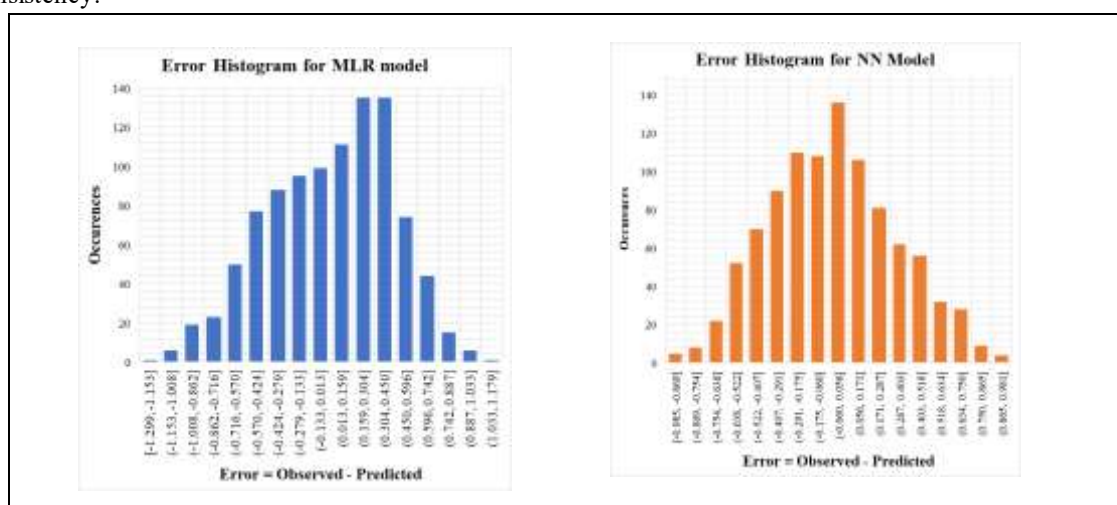


Figure 12 Error Histogram

Figure 13 compares the predicted and observed SDI values for MLR and ANN models. The MLR model shows greater deviation and variability, especially during validation, indicating moderate accuracy. In contrast, the ANN model closely follows observed values across both phases, capturing trends and fluctuations more effectively.

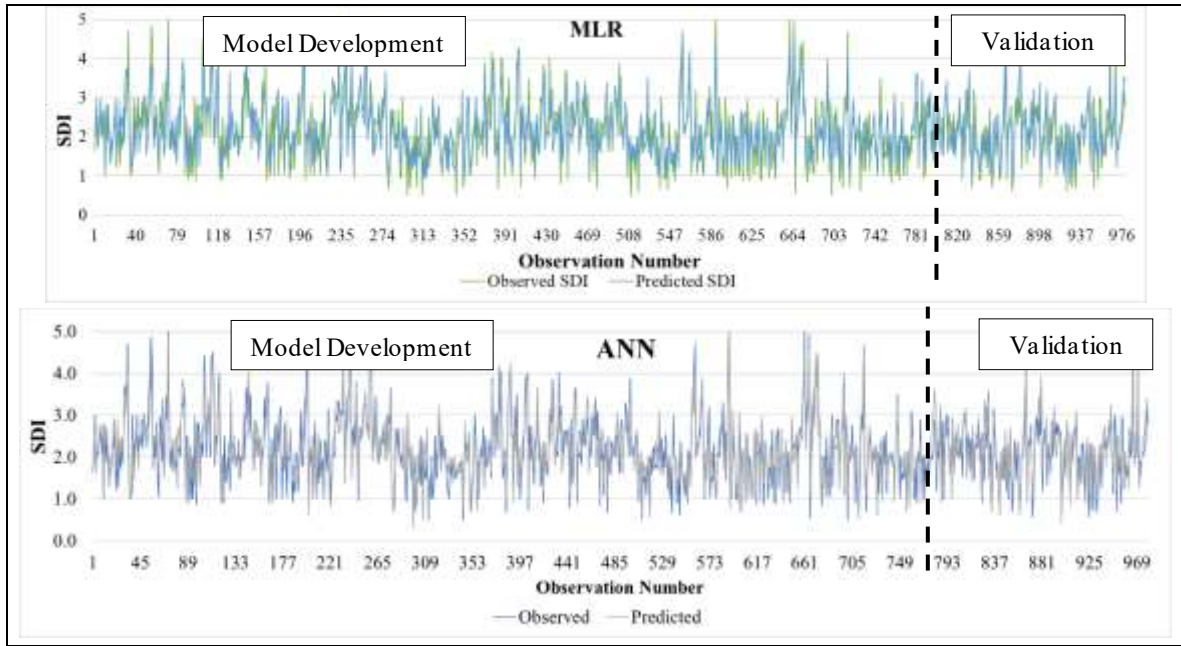


Figure 13 Comparison between predicted and observed SDI under MLR and ANN

#### 4.5 Sensitivity Analysis

Table 7 presents the sensitivity index for each variable in the developed models. IRI is the most influential predictor, with the highest sensitivity in both MLR (0.78) and ANN (0.76). Age and Rainfall show similar influence across models, though MLR gives Age more weight (0.38 vs. 0.34) and less to Rainfall (0.21 vs. 0.24) than ANN. Temperature has a moderate impact (MLR: 0.37, ANN: 0.36), while CV shows the least sensitivity (MLR: 0.09, ANN: 0.13), likely due to maintenance interventions in high-traffic sections.

Table 7 Sensitivity Index in Variables

	IRI	Age	Rainfall	Temp. Diff.	CV
MLR	0.78	0.38	0.21	0.37	0.09
ANN	0.76	0.34	0.24	0.36	0.13

#### 4.6. Discussion

The study developed prediction models using all available and verified data from the national database. However, the findings are constrained by the limited availability and completeness of reliable datasets in Nepal. The absence of detailed pavement classification records restricted the analysis to a generalized category of flexible pavements. Further disaggregation by surface type would have significantly reduced the dataset and compromised the statistical robustness of the models. Similarly, the limited number of permanent traffic count stations constrained the study to road sections with verified traffic and roughness data, despite the presence of a larger number of road sections in the SRN. The use of climatic data from the nearest DHM stations introduces another potential source of uncertainty, as Nepal's complex topography causes substantial variation in rainfall and temperature over short distances. Nevertheless, the DHM remains the only institution maintaining continuous and standardized climatic datasets, and using the nearest available stations ensured methodological consistency and reliability under current data constraints.

Despite these limitations, the selected road sections span diverse physiographic and climatic regions, including the Terai, mid-hill, and mountain zones, capturing a broad range of environmental and traffic conditions. Therefore, the developed models are considered reasonably representative of Nepal's flexible pavement performance at a national scale within the bounds of existing data.

## 5. Conclusion

The study developed and evaluated two predictive models: MLR and ANN, to forecast the SDI of Nepal's national highway pavement network using five key variables: IRI, pavement age, annual rainfall, annual temperature difference, and commercial vehicle traffic. Using a comprehensive dataset covering 157 road sections over ten years (2012–2022), the models were trained and validated to assess their performance and predictive capabilities. The correlation analysis showed no signs of multicollinearity, validating the inclusion of all variables. MLR analysis was conducted in Microsoft Excel, which assessed statistical significance through ANOVA,  $R^2$  values, and regression coefficients. The MLR model demonstrated a dependable predictive performance with an  $R^2$  of 0.735 during development and 0.740 in validation, explaining approximately 73% of the variance in SDI. All five predictors were statistically significant, with IRI and pavement age having the most substantial impact. Despite its interpretability and simplicity, MLR showed limitations in capturing non-linear interactions between variables. ANN modeling used a MLP architecture implemented in TensorFlow and the Keras library of Python programming, which involved a number of iterations throughout varied network architectures to achieve the optimal architecture with the least MSE and highest  $R^2$  employing ReLU activation and the Adam optimizer. The research evaluated multiple Neural Network architectures, starting with simple single-layer networks and progressing to DNNs with up to four hidden layers. The optimal ANN model, the 5-232-1 model with 104 epochs, significantly outperformed MLR across all evaluation metrics. It achieved an  $R^2$  of 0.809 during training and 0.816 during validation, indicating stronger predictive accuracy and generalization. The ANN's capacity to model complex, non-linear relationships between pavement distress and influencing factors resulted in improved estimation accuracy, reduced MSE, and narrower prediction error distributions. Sensitivity analysis revealed that IRI is the most influential predictor in both models, followed by pavement age and rainfall. Commercial vehicle traffic showed the least sensitivity, likely due to offsetting effects of maintenance on high-traffic routes.

The findings of this study offer actionable insights for the DoR in Nepal. By integrating ANN-based predictive models into the existing PMS, the DoR can improve maintenance planning, optimize budget allocation, and reduce reliance on labor-intensive condition assessments. The enhanced predictive accuracy allows for proactive intervention. Moreover, routine incorporation of variables such as IRI, rainfall, temperature range, and commercial vehicle traffic can support data-driven decision-making and reduce maintenance costs. Policymakers could also consider expanding traffic count stations and improving climatic monitoring to further strengthen model reliability and facilitate long-term infrastructure planning. Future studies could explore incorporating additional variables such as subgrade strength, construction quality, or socio-economic factors, and test deep learning architectures for further performance gains.

## 6. References

- Abaza, K. A. (2006). Iterative linear approach for non-linear non-homogenous stochastic pavement management models. *Journal of Transportation Engineering*, 132(3), 244–256.
- Abaza, K. A., Ashur, S. A., & Al-Khatib, I. A. (2004). Integrated pavement management system with a Markovian prediction model. *Journal of Transportation Engineering*, 130(1), 24–33. [https://doi.org/10.1061/\(ASCE\)0733-947X\(2004\)130:1\(24\)](https://doi.org/10.1061/(ASCE)0733-947X(2004)130:1(24))
- Adeli, H. (2001). Neural networks in civil engineering: 1989–2000. *Computer-Aided Civil and Infrastructure Engineering*, 16(2), 126–142.
- Anyala, M., Odoki, J. B., & Baker, C. J. (2014). Hierarchical asphalt pavement deterioration model for climate impact studies. *International Journal of Pavement Engineering*, 15(3), 251–266. <https://doi.org/10.1080/10298436.2012.687105>
- Arhin, S. A., & Noel, E. C. (2014). *Predicting pavement condition index from international roughness index in Washington, DC*.
- Ashrafian, A., Taheri Amiri, M. J., Masoumi, P., Asadi-shiadeh, M., Yaghoubi-chenari, M., Mosavi, A., & Nabipour, N. (2020). Classification-based regression models for prediction of the mechanical properties of roller-compacted concrete pavement. *Applied Sciences*, 10(11), 3707. <https://doi.org/10.3390/app10113707>

- Bosurgi, G., & Trifirò, F. (2005). A model based on artificial neural networks and genetic algorithms for pavement maintenance management. *International Journal of Pavement Engineering*, 6(3), 201–209.
- Chang, C.-L., & Liao, C.-S. (2012). Parameter sensitivity analysis of artificial neural network for predicting water turbidity. *International Journal of Geological and Environmental Engineering*, 6(10), 657–660.
- Department of Road. (2023). *Highway Management Information System – ICT Unit*. <https://www.dor.gov.np/home/page/hims-and-ict-unit>
- Department of Roads. (2022). *Statistics of National Highway*. [https://ssm.dor.gov.np/road\\_network/getNationCategoryAndPavement/](https://ssm.dor.gov.np/road_network/getNationCategoryAndPavement/)
- Department of Roads (DoR). (2007, April). HMIS Newsletter Vol. 22. *Highway Management Information System*.
- Department of Roads, & Maintenance Branch. (2005). *Standard Procedure for Periodic Maintenance Planning*.
- Domitrović, J., Dragovan, H., Rukavina, T., & Dimter, S. (2018). Application of an artificial neural network in pavement management system. *Tehnički Vjesnik*, 25(Supplement 2), 466–473.
- Durango-Cohen, P. L., & Tadeipalli, N. (2006). Using advanced inspection technologies to support investments in maintenance and repair of transportation infrastructure facilities. *Journal of Transportation Engineering*, 132(1), 60–68.
- Elshamy, M. M. M., Tiraturyan, A. N., Uglova, E. V., & Zakari, M. (2020). Development of the non-destructive monitoring methods of the pavement conditions via artificial neural networks. *Journal of Physics: Conference Series*, 1614(1), 012099.
- Ferreira, A., Picado-Santos, L., & Antunes, A. (1999). Pavement performance modelling: State of the art. *Proceedings of Seventh International Conference on Civil and Structural Engineering Computing*, 157–264.
- Fwa, T. F., Chan, W. T., & Hoque, K. Z. (2000). Multi-objective optimization for pavement maintenance programming. *Journal of Transportation Engineering*, 126(5), 367–374.
- Georgiou, P., Plati, C., & Loizos, A. (2018). Soft Computing Models to Predict Pavement Roughness: A Comparative Study. *Advances in Civil Engineering*, 2018, 1–8. <https://doi.org/10.1155/2018/5939806>
- Glorot, X., Bordes, A., & Bengio, Y. (2011). Deep sparse rectifier neural networks. *Proceedings of the Fourteenth International Conference on Artificial Intelligence and Statistics*, 315–323.
- Gong, H., Sun, Y., Hu, W., Polaczyk, P. A., & Huang, B. (2019). Investigating impacts of asphalt mixture properties on pavement performance using LTPP data through random forests. *Construction and Building Materials*, 204, 203–212. <https://doi.org/10.1016/j.conbuildmat.2019.01.198>
- Haykin, S. (1998). *Neural networks: a comprehensive foundation*. Prentice Hall PTR.
- Highway Management Information System-Information & Communication Technology (HMIS-ICT) Unit. (2022). *Traffic, Surface Distress and Road Roughness Surveys on Strategic Road Network*.
- Kerali, H. G. R., Odoki, J. B., & Stannard, E. E. (2000). Overview of HDM-4. *The Highway Development and Management Series, Volume One, World Road Association, PIARC. World Bank, Washington DC, USA*.
- Kulkarni, R. B., Miller, D., Ingram, R. M., Wong, C.-W., & Lorenz, J. (2004). Need-based project prioritization: alternative to cost-benefit analysis. *Journal of Transportation Engineering*, 130(2), 150–158.
- Kulkarni, R. B., & Miller, R. W. (2003). Pavement management systems: Past, present, and future. *Transportation Research Record*, 1853(1), 65–71.
- LeCun, Y., Bengio, Y., & Hinton, G. (2015). Deep learning. *Nature*, 521(7553), 436–444.
- Mathavan, S., Kamal, K., & Rahman, M. (2015). A review of three-dimensional imaging technologies for pavement distress detection and measurements. *IEEE Transactions on Intelligent Transportation Systems*, 16(5), 2353–2362. <https://doi.org/10.1109/TITS.2015.2428655>
- Meneses, S., Ferreira, A., & Collop, A. (2013). Multi-objective decision-aid tool for pavement management. *Proceedings of the Institution of Civil Engineers-Transport*, 166(2), 79–94.
- Mosa, A. M. (2017). Neural network for flexible pavement maintenance and rehabilitation. *Applied Research Journal*, 3(4), 114–129.
- Neter, J., Kutner, M. H., Nachtsheim, C. J., & Wasserman, W. (1996). *Applied linear statistical models*.

- Picado-Santos, L., Ferreira, A., Antunes, A., Carvalheira, C., Santos, B., Bicho, M., Quadrado, I., & Silvestre, S. (2004). Pavement management system for Lisbon. *Proceedings of the Institution of Civil Engineers-Municipal Engineer*, 157(3), 157–165.
- Sanabria, N., Valentin, V., Bogus, S., Zhang, G., & Kalthor, E. (2017). *Comparing neural networks and ordered probit models for forecasting pavement condition in New Mexico*.
- Sazlı, M. H. (2006). A brief review of feed-forward neural networks. *Communications Faculty of Sciences University of Ankara Series A2-A3 Physical Sciences and Engineering*, 50(01).
- Shakya, M., Sasai, K., & Kaito, K. (2023). Application of Markov Deterioration Hazard Model for Pavement Deterioration Forecasting of Strategic Road Networks in Nepal. *2<sup>nd</sup> International Conference on Integrated Transport for Sustainable Mobility*, 59–70.
- Shrestha, A., & Mahmood, A. (2019). Review of deep learning algorithms and architectures. *IEEE Access*, 7, 53040–53065.
- Shrestha, S., & Khadka, R. (2021). Assessment Of Relationship Between Road Roughness and Pavement Surface Condition. *Journal of Advanced College of Engineering and Management*, 6, 2021. <https://doi.org/10.3126/jacem.v6i0.38357>
- Sigdel, T., & Pradhananga, R. (2021). *Development of IRI Prediction Model for National Highways of Nepal*. 10, 2350–8906.
- Sigdel, T., Pradhananga, R., & Shrestha, S. (2024). Artificial Neural Network-based model to predict the International Roughness Index of national highways in Nepal. *Transportation Research Interdisciplinary Perspectives*, 25, 101128.
- Wang, W., Qin, Y., Li, X., Wang, D., & Chen, H. (2017). Comparisons of Faulting-Based Pavement Performance Prediction Models. *Advances in Materials Science and Engineering*, 2017, 1–9. <https://doi.org/10.1155/2017/6845215>
- Wong, W. G., He, G. P., & Luk, S. T. (2003). Development of road management systems in China. *Proceedings of the Institution of Civil Engineers-Transport*, 156(4), 179–188.
- Yang, X., Guan, J., Ding, L., You, Z., Lee, V. C. S., Hasan, M. R. M., & Cheng, X. (2021). Research and applications of artificial neural network in pavement engineering: a state-of-the-art review. *Journal of Traffic and Transportation Engineering (English Edition)*, 8(6), 1000–1021.
- Zakeri, H., Nejad, F. M., & Fahimifar, A. (2017). Image based techniques for crack detection, classification and quantification in asphalt pavement: a review. *Archives of Computational Methods in Engineering*, 24, 935–977. <https://doi.org/10.1007/s11831-016-9194-z>